

# Secretory Conservation in Insulin Producing Cells: Is There a System-Level Law of Mass Action in Biology?

Firdos and Aditya Mittal\*

Cite This: *ACS Omega* 2023, 8, 37573–37583

Read Online

ACCESS |



Metrics &amp; More



Article Recommendations

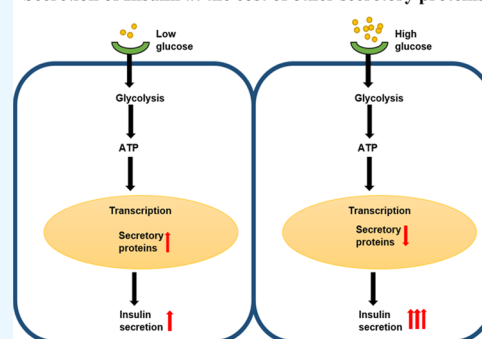


Supporting Information

**ABSTRACT:** Altered secretion of insulin from pancreatic  $\beta$ -cells can manifest into disorders. For example, a lack of endogenously produced and/or secreted insulin results in Type 1 diabetes (and other associated subtypes). Pancreatic  $\beta$ -cells are the endocrine secretory cells that promote insulin secretion in response to glucose stimulation. Secretion in response to extracellular triggers is an interplay among various signaling pathways, transcription factors, and molecular mechanisms. The Mouse Insulinoma 6 (MIN6) cell line serves as a model system for gaining mechanistic insights into pancreatic  $\beta$ -cell functions. It is obvious that higher glucose consumption and increased insulin secretion are correlated. However, it has been reported that intracellular ATP levels remain  $\sim$  constant beyond the extracellular glucose (EG) concentration of 10 mM. Therefore, any cause–effect relationship between glucose consumption (GC) and enhanced insulin secretion (eIS) remains unclear. We also found that total cellular

protein, as well as total protein content in the culture “supernatant,” remains constant regardless of varying EG concentrations. This indicated that eIS may be at the cost of (a) intracellular synthesis of other proteins and (b) secretion of other secretory proteins, or both (a) and (b), somehow coupled with GC by cells. To gain insights into the above, we carried out a transcriptome study of MIN6 cells exposed to hypoglycemic (HoG = 2.8 mM EG) and hyperglycemic (HyG = 25 mM EG) conditions. Expression of transcripts was analyzed in terms of Fragments Per Kilobase of transcript per Million mapped reads and Transcripts Per Million (FPKM and TPM) as well as values obtained by normalizing w.r.t. “ $\sum$ (FPKM)” and “ $\sum$ (TPM).” We report that HyG extracellular conditions lead to an  $\sim$ 2-fold increase in insulin secretion compared to HoG measured by the enzyme-linked immunosorbent assay (ELISA) and transcripts of secreted proteins as well as their isoforms decreased in HyG conditions compared to HoG. Our results show for the first time that eIS in HyG conditions is at the cost of reduced transcription of other secreted proteins and is coupled with higher GC. The higher GC at increased extracellular glucose also indicates a yet undiscovered role of glucose molecules enhancing insulin secretion, since ATP levels resulting from glucose metabolism have been reported to be constant above an EG concentration of 10 mM. While extrapolation of our results to clinical implications is ambitious at best, this work reports novel cellular level aspects that seem relevant in some clinical observations pertaining to Type 1 diabetes. In addition, the conservatory nature of cellular secretions in insulin-secreting cells, discovered here, may be a general feature in cell biology.

## Secretion of Insulin at the cost of other secretory proteins



## INTRODUCTION

Cellular secretion is central to biology. Enhanced secretion of certain proteins resulting from regulatory processes and/or in response to environmental triggers is a general feature of all cells. From this perspective, one of the most important naturally occurring systems is glucose-stimulated insulin secretion (GSIS) by specific cells in vertebrates. The inability to produce and/or secrete insulin, presumably due to the immune-mediated destruction of pancreatic  $\beta$  cells, gives rise to a disorder such as Type 1 diabetes (T1D) predominantly at a young age. This is arguably induced by genetic and environmental factors.<sup>1</sup> Despite the discovery of T1D  $\sim$ 47 years ago and recognition of the fact that it is one of the major causes of life-long morbidity and eventual mortality, there is still no cure available for this disorder.<sup>2,3</sup> The International Diabetes Federation (IDF, 2021) estimated 537 million cases of diabetes in 2021 and predicted an increase of approximately

783 million by 2045 worldwide.<sup>4</sup> Although T1D accounts for 5–10% of total diabetes cases, this disorder causes severe comorbidities such as micro- and macrovascular diseases with other physiological problems having long-term consequences.<sup>3,5</sup> Clinical diagnosis of T1D is often followed by “honeymoon phases” in patients, in which exogenous insulin administration somehow allows a temporary “rescue” of physiological insulin secretion—this fades away after some days or several months. Apart from the “honeymoon phases”

Received: August 16, 2023

Accepted: September 19, 2023

Published: September 27, 2023



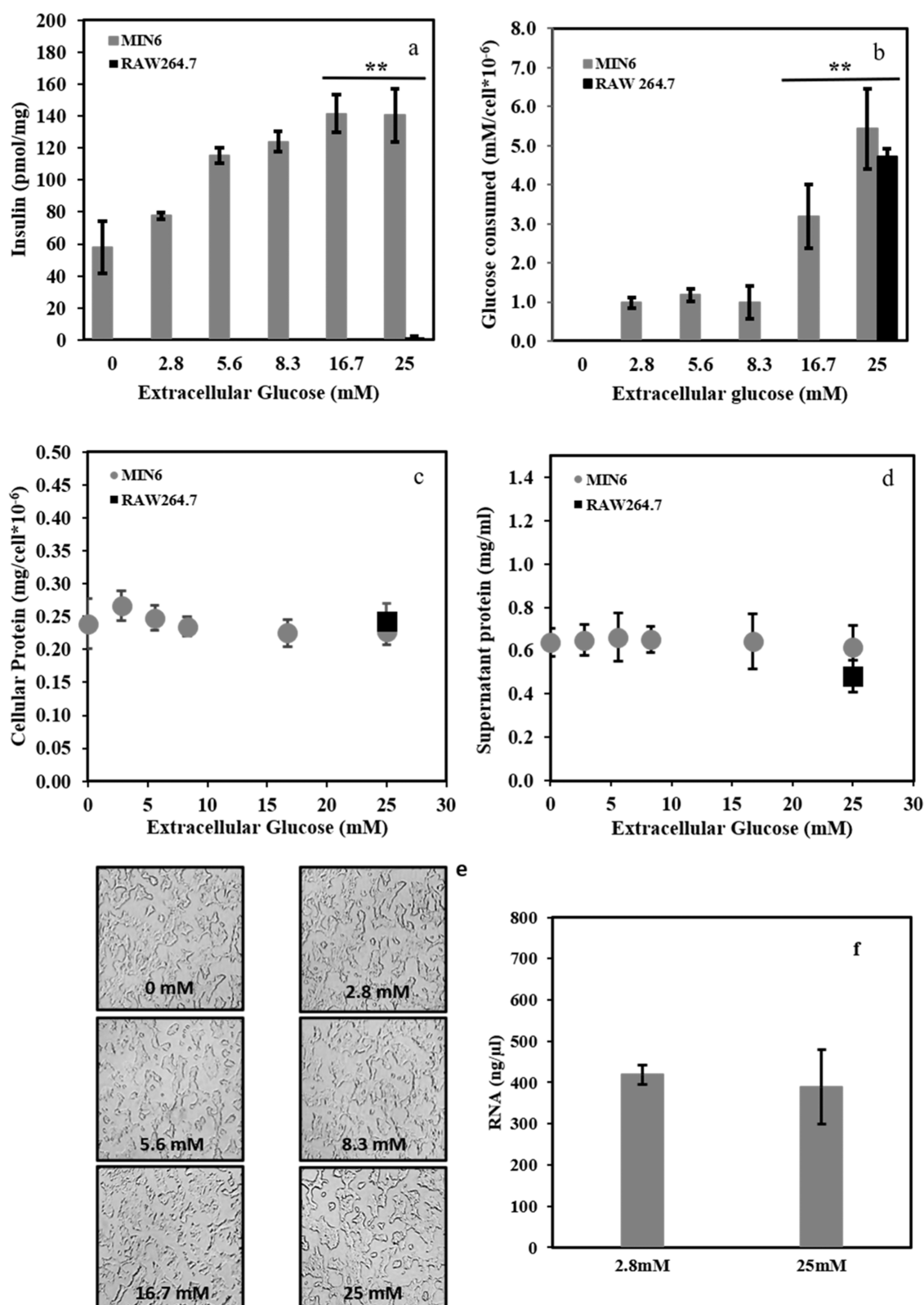


**Figure 1.** Insulin secretion independent of total protein. (a) Increasing insulin secretion ( $p \sim 0.003$  between 2.8 and 25 mM) coupled with (b) increasing consumption of glucose ( $p \sim 0.002$  between 2.8 and 25 mM) as a result of increasing extracellular glucose. (c, d) Cellular and supernatant proteins. (e) Representative images of MIN6 cells; cellular morphology appears independent of extracellular glucose concentrations. All data are shown as mean  $\pm$  SD ( $n = 3$ ). (f) Isolated similar RNA concentrations at hypoglycemic (HoG) and hyperglycemic (HyG) glucose concentrations. Cellular RNA for cells exposed to both extracellular glucose is similar.

associated with T1D, there are other clinical forms of temporary T1D-like disorders. For example, gestational

diabetes in pregnant females requires exogenous insulin administration—often, physiological insulin secretion is some-

how restored after childbirth. Regardless of T1D or T1D-like temporary conditions, maintenance of normoglycemia is a major challenge in patients with problems with insulin synthesis and/or secretion. Glycaemic variability causes hyperglycemia, HyG >7.8 mM/L (rise in blood sugar), and hypoglycemia, HoG <3.3 mM/L (decrease in blood sugar),<sup>6</sup> thereby increasing clinical complications not only in diabetic<sup>7</sup> but also in nondiabetic patients.<sup>8</sup> Thus, mechanistic studies on GSIS in cellular systems are important for insights into T1D as well as T1D-like temporary conditions. Interestingly, GSIS also allows for the possibility of exploring general secretory mechanisms in cell biology due to well-characterizable experimental conditions pertaining to the synthesis and secretion of a specific protein. Therefore, in this work, we utilize the Mouse Insulinoma Cells 6 (MIN6) cultures, which are a well-established model system, to investigate GSIS by pancreatic  $\beta$ -cells.<sup>9,10</sup>

Here, it becomes pertinent to emphasize that in GSIS systems, such as MIN6 cells, it is generally assumed that intracellular glucose serves as a nutrient for survival/growth and extracellular glucose serves as an environmental trigger for enhancing synthesis + secretion of a particular protein (insulin in this case).<sup>10</sup> In cell biology, such coupling of a single molecular species serving multiple purposes is generally common to several regulatory mechanisms (e.g., signaling, feedback mechanisms via transcriptional controls, etc.). Directed by such regulatory mechanisms, thousands of genes are transcribed, eventually leading to the synthesis of a variety of cellular, secretory, and membrane proteins essential for cellular survival and propagation.<sup>11</sup> Of these, secretory proteins must pass through secretory pathways involving the Golgi complex, ER, and plasma membranes subsequent to post-translational modifications. The eventual secretion of particular proteins, triggered by extracellular stimuli, is then a combined effect of the secretory pathways and cellular signaling cascades.<sup>12</sup> In fact, it may be argued that secreted proteins require the highest energetic investments from cells toward their processing as compared to other proteins.<sup>13</sup> If not by anything else, the extra step of proper intracellular packaging of proteins for their eventual secretion may impose demands on cells that can compromise the synthesis and production of other cellular proteins. In such a case, it becomes reasonable to assume that HyG extracellular conditions for MIN6 (and alike) cells would favor higher intracellular energy production, e.g., in the form of ATP, resulting from higher consumption of glucose in order to meet higher insulin secretion requirements. However, it has been reported that ATP levels (indicative of overall intracellular energy supply) remain constant beyond the extracellular glucose concentration of 10 mM in human, rat, and mouse islet cells.<sup>14,15</sup> This phenomenon could potentially impose an additional metabolic load on cells during heightened insulin secretion. Further, it is interesting to note that ATP also plays a crucial role in the acidification of insulin-carrying vesicles and insulin exocytosis,<sup>16,17</sup> in addition to its general role as the currency of intracellular energy. Thus, there is an obvious limit to intracellular energy generation, independent of the availability of metabolic energy sources, such as glucose, beyond a certain amount.

Then, how do cells enhance the synthesis, followed by secretion, of specific molecules such as insulin? To answer this question, we exposed MIN6 cells to HoG and HyG conditions to examine possible relationships between variable levels of insulin secretion and overall cellular protein content as well as

protein content in cell “supernatant” (which includes total secreted protein) under highly controlled culture conditions without the interference of media components. Further, we carried out comprehensive whole transcriptome analyses of MIN6 cells exposed to both HoG and HyG conditions, with the latter resulting in more than twice the insulin secreted compared to the former. We report, for the first time, that enhanced insulin secretion is at the cost of other secretory proteins but not other cellular proteins. Our results show that this compensatory cost of other secretory proteins for enhanced GSIS is regulated at three levels: transcriptional, translational, and secretory-vesicle (insulin granules) preparation. Our findings, while being directly relevant to the important area of T1D and T1D-like disorders, may also indicate a general mechanism of the conservation of total secretory proteins in cell biology.

## RESULTS

**GSIS Enhances Insulin Secretion without Affecting Total Cellular Proteins.** Figure 1a shows that insulin secretion by MIN6 cells, bathed in medium-free predominantly buffer solution, was enhanced with varying extracellular glucose concentrations—increasing by more than twice under HyG (>~8 mM) conditions compared to HoG (<~3 mM). Note that even in the absence of glucose, some insulin secretion (slightly lower than HoG conditions) was still observed. This is due to residual insulin secretion resulting from the cells while they were in a regular culture medium—since insulin measurements are carried out within an hour of incubation in the predominantly buffer-containing cell bathing solution. This residual insulin secretion in the absence of glucose also gave us the first indications of translational and/or post-translational and/or secretory mechanisms dominating over transcriptional and/or synthesis mechanisms during GSIS. As a negative control experiment, RAW264.7 showed no insulin secretion even at the highest extracellular glucose concentrations (almost invisible black bar shown at 25 mM extracellular glucose in Figure 1a). The proportion of insulin secretion was examined in relation to both the cellular protein and supernatant protein. The assessment involved measuring insulin secretion in micrograms per milligram of cellular protein, as illustrated in Appendix A. We contrasted the proportion of insulin with the proportion of the entire supernatant protein per milligram of cellular proteins. Initially, we computed the overall supernatant protein with milligrams of cellular protein in Appendix B, followed by determining the specific fraction attributed to insulin secretion within the supernatant protein, as detailed in Appendix C. Asserting that the increase in insulin secretion magnifies the metabolic workload, resulting in a decline in the levels of other secreted proteins found in the supernatant. This implies a significant decrease in the overall protein content within the supernatant, attributable to heightened metabolic demands. Although the proportion of secreted insulin constitutes less than 1% when compared to both secreted and cellular proteins, as demonstrated in Appendices A and C, there are two potential reasons for this observation. First, the amount of secreted protein is relatively low. Second, we introduced 1 mg/mL BSA into the KRBH buffer to stabilize the reaction during our experimental hour-long duration. Such a high concentration of protein in the supernatant might mask the presence of secreted proteins, thereby leading to an apparent decrease in the amount of secreted insulin within the supernatant. Figure 1b shows that glucose consumption per

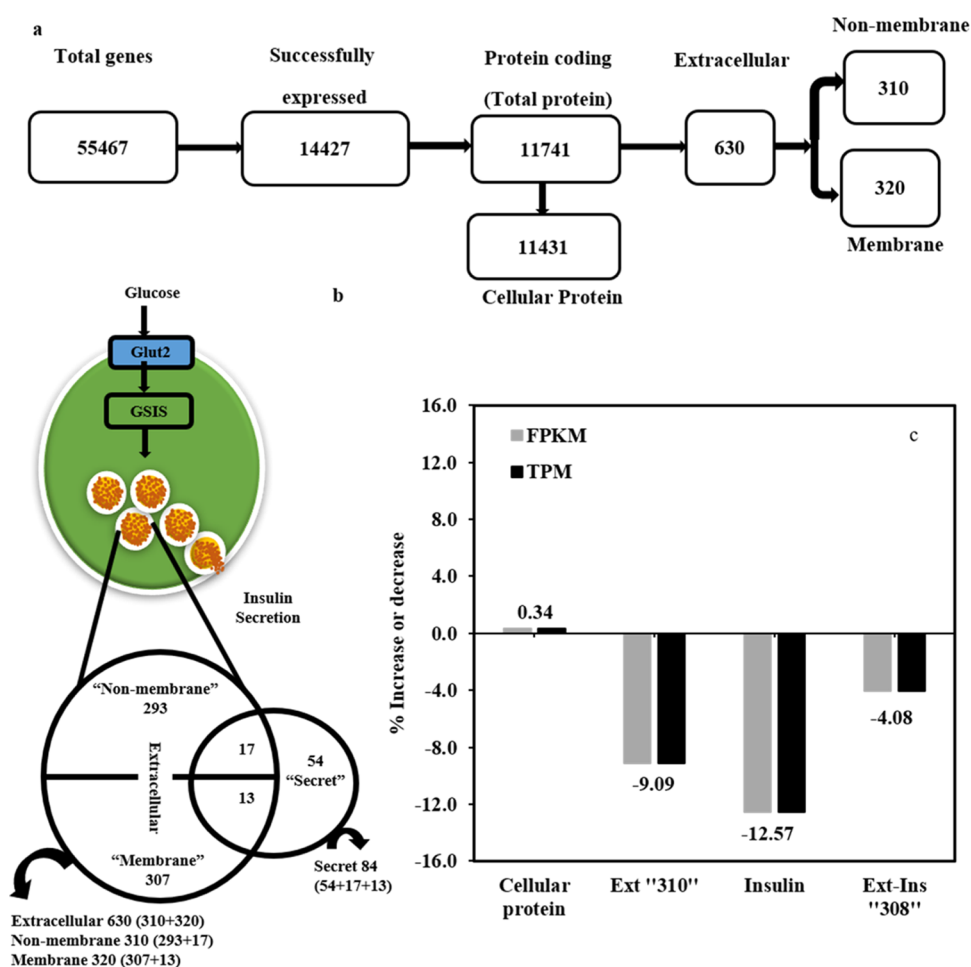


**Figure 2.** (a) Flow diagram of transcriptome analysis and (b) distribution of extracellular, secretory, and membrane proteins. (c) Transcriptome changes in cellular protein and extracellular and/or secreted proteins (including/excluding insulin) of total protein transcripts without insulin at high glucose; results from the value of transcripts as in TPM and FPKM are shown in Supporting Table 1.

cell increased under HyG extracellular conditions. However, it is clear that while insulin secretion appears to be well correlated with extracellular glucose concentrations (Figure 1a), the correlation between glucose consumed by cells and extracellular glucose concentrations is not that trivial (Figure 1b). Further, glucose consumption by RAW264.7 cells (black bar) at HyG conditions, despite no insulin secretion, was comparable to the glucose consumed by MIN6 cells under similar conditions.

While the results obtained in Figure 1a,b were similar to those reported earlier in the literature,<sup>10,11</sup> Figure 1c shows cellular protein per cell, the first novel result obtained in our experiments. The total cellular protein content of MIN6 cells was independent of extracellular glucose concentrations and similar for all glucose concentrations. Glucose consumption has been further examined in Appendix D, expressed as moles per cell. In fact, it was interesting to note that even RAW264.7 cells had almost identical total cellular protein. In the context of literature, this is a novel discovery, probably undiscovered to date, since the total cellular protein in cultures, rather than cellular protein content per cell, is generally measured and reported. Our results indicate that the maintenance of total cellular protein may be a general feature in cell biology. Even more interesting was the result that total “supernatant” protein, which included secreted proteins, was also independent of extracellular glucose concentrations, as shown in Figure 1d.

The calculation for Figure 1d has been performed on a per cell basis using the supernatant protein data from Appendix E. Clearly, enhanced insulin production and/or secretion by MIN6 cells were somehow being compensated by under-production/secretion of other cellular and/or secreted proteins. Figure 1e shows that there were no observable morphological variations in MIN6 cells incubated with predominantly buffer solutions containing different extracellular glucose concentrations. Here, it is important to note that to date, cell biology across the world relies on an “intuitive” feel of how cells appear in cell cultures to experimentalists. Thus, if total cellular protein per cell or “supernatant” protein is assumed to be the indicator of the “health” of cells, the lack of morphological variations observed by us correlates well with the “intuitive” visual interpretations in general wet-experimental cell biology. More importantly, our results show that enhanced insulin secretion in GSIS was due to a decrease in the synthesis of other proteins or specifically at the cost of other secreted proteins only. Either or both of the above possibilities were also supported by the fact that while glucose consumption increases with an increase in extracellular glucose concentration, it does not increase the available cellular energy in the form of ATP beyond the extracellular glucose concentration of 10 mM.<sup>14,15</sup>

**Total RNA Content and Whole Cell Transcriptome Analyses.** To explore possible (re)allocation of cellular

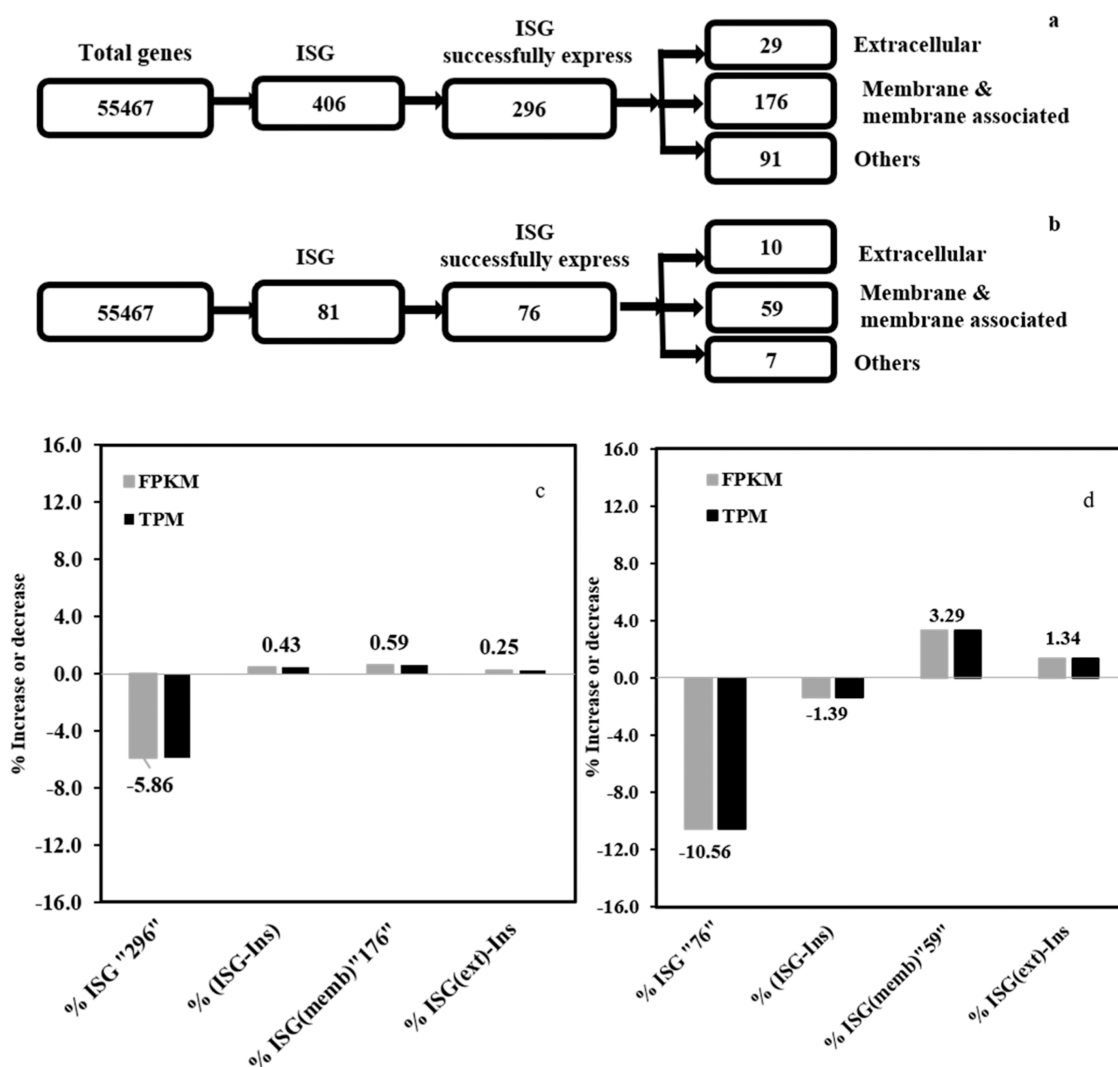


**Figure 3.** (a) Flow diagram showing that the number of genes successfully expressed is "296", previously found in literature 2007, 09, 12, and 18. (b) Flow diagram showing 76 proteins of insulin secretory granules (81 from highly confident literature on ISG proteins). (c) There was no considerable high change in the % of ISG of total protein-coding transcripts without insulin at high glucose. (d) There were no considerably high changes in the % of ISG of protein-coding transcripts without insulin; results from the value of transcripts as in TPM and FPKM are shown in Supporting Tables 4 and 5.

resources toward enhanced insulin secretion in GSIS, we decided to focus on specific HoG (2.8 mM extracellular glucose) and HyG (25 mM extracellular glucose) conditions. In addition to the earlier total cellular protein content being similar, we report our next novel finding—Figure 1f shows that total cellular RNA content was also similar at HoG and HyG conditions. This result now directed us to carry out whole cellular transcriptome studies of MIN6 cells exposed to HoG and HyG conditions.

Figure 2a shows that a total of 55,467 genes were identified in MIN6 transcriptomes, of which 14,427 were successfully expressed (in both HoG and HyG samples). Of these 14,427 genes, 11,741 were identified as protein-coding, in which 11,431 belonged to cellular proteins. Due to our interest in secreted proteins, we first identified that 630 of these genes were extracellular (see the Materials and Methods section). Of these 630 extracellular genes, 310 correspond to non-membrane (i.e., may be assumed to be soluble proteins that were secreted) and 320 correspond to membrane proteins (i.e.,

may be assumed to be extracellular membrane proteins including those associated with secreted vesicles).<sup>18</sup>

In transcriptome studies, we have further filtered out a total of 630 extracellular proteins (nonmembrane 310 and membrane 320) from successfully expressed protein-coding genes, which have been shown in the outline flow in Figure 2a. The vein diagram in Figure 2b demonstrates the distribution of extracellular secreted proteins. Next, we have done a comparative analysis of the increase/decrease of transcripts in the form of percentage difference of  $\sum$ FPKM and  $\sum$ TPM at two different concentrations of glucose HoG (2.8 mM) and HyG (25 mM) of secreted extracellular (310 nonmembrane) proteins. We can see that at a high concentration of glucose, cells decrease the expression of the transcript of extracellular secreted (nonmembrane) proteins with/without insulin in Figure 2c. From these results, we can see that the insulin transcript also decreases with increasing insulin secretion at high glucose levels because insulin translation and secretion do not directly reflect insulin transcriptional products. The results depicting the non-normalized values of the transcript in Figure

2c have been displayed in Appendix F. Supporting Table 1 shows the transcript values of Figure 2c in the form of TPM and FPKM. This shows that transcripts of extracellular proteins decrease at HyG 25 mM w.r.t HoG 2.8 mM of glucose.

Various isoforms are produced due to the result of alternate splicing. Here, we have filtered out a total of 1376 extracellular proteins (nonmembrane 632 and membrane 744) from successfully expressed protein-coding isoforms, which have been shown in the outline flow in Appendix G in Figure (a) and Venn diagram in (b). Isoform analysis has also been done in the same way as the analysis of the transcripts, and the same results have been found in the isoform, which is demonstrated in Appendix G. We have found the same result and way of decreasing as in potential transcripts. Isoform's FPKM and TPM values are given in Supporting Table 2. These results also favor cells decreasing the extracellular protein isoforms at HyG.

**Insulin Secretory Granules (ISGs).** Proteins of insulin secretory granules are not only a member of the insulin granules but also participate in the biogenesis of insulin and the secretion process inside the secretory granule.<sup>19,20</sup> ISG proteins were identified initially in 1982 with the help of the density gradient centrifugation method.<sup>21</sup> Later studies were performed by density gradient centrifugation, mass spectrophotometry, and immune-affinity-based methods. We collected the proteomic profile of the ISG of  $\beta$  cells in Rat insulinoma cells (INS1) from literature studies. Only four studies have complete data on proteins of insulin granules until this period.<sup>22–25</sup> Only five genes identified common *Chga*, *Cpe*, *Ins1*, *Ins2*, and *Pcsk2* in all four studies mentioned in the previous review also.<sup>26</sup> Figure 3a,3b has shown the outline flow of the number of insulin secretory proteins from all four literature studies<sup>22–25</sup> and the last literature based on protein correlation profiling.<sup>25</sup> Detailed ISG proteins are given in Table 1 and Supporting Table 3.

Figure 3c,d shows the changes in the transcripts of total granule proteins and the percentage ISG of total protein-coding transcripts. Figure 3c shows that ISG proteins from previous studies by Schwartz et al., Hickey et al., and Brunner et al. are based on the gradient purification method, which might have polluted with membrane and membrane protein fragments from the ER to GC passage.<sup>22–25</sup> Figure 3d shows 81 ISG proteins identified by Li et al. by correlation profiling based on elucidation distance to reduce the contamination of the other proteins in the identification of ISG proteins.<sup>25</sup> So, the results were analyzed for these genes separately. The transcripts decrease and increase with and without insulin, as shown in Figure 3c,d. The values of transcripts as in TPM and FPKM are shown in Supporting Tables 4 and 5. These results show that transcripts of extracellular (intravesicular) proteins of ISG and membrane-associated proteins do not change.

## DISCUSSION

The major finding of our work is that at high glucose concentrations, insulin secretion is enhanced by reducing transcripts of extracellular/secreted proteins. On the one hand, it is interesting that hyperglycemic treatment reduces transcription levels of secretory proteins in insulin producing MIN6 cells. On the other hand, it may be argued that at this point, there is no direct evidence showing how the transcriptional suppression of secretory proteins occurs or how this transcriptional suppression is related to the induction of insulin secretion in the cells with hyperglycemia. While further work is required for unambiguous resolution of the above, we provide

**Table 1. Comprehensive Set ISG "328" of a Total "406" after Removing Common Genes from the Superset of Supporting Table 4<sup>a</sup>**

s. no.	ISG proteins	number	D/ND/NP
1	Abhd17b, Ace, Acl, Actb, Actr1a, Adam22, Aga, Aldoa, Angptl8, Anxa1, Anxa4, Ap2a1, App, Aprt, Arcn1, Arf6, Arfp1, Auhgap1, Atr8b, Arsb, Asahi, Atpla1, Atp5a1, Atp5b, Atp5c1, Atp6ap1, Atp6ap2, Atp6v0c, Atp6v0d1, Atp6v1a, Atp6v1b, Atp6v1c, B3gat3, B4gat3, Btf3l4, Calc, Cand1, Cant1, Cap1, Caprin1, Casc4, Cct3, Cct4, Cct5, Chga, Chgb, Ckap4, Clint1, Cltc, Clu, Cnp, Copb1, Cope1, Cpd, Cpe, Cpm1, Crmp1, Csnk2a1, Cst3, Csth, Ctbs, Ctsb, Ctsd, Cysl, Dag1, Dbn1, Dnaic5, Dpp7, Eef1a1, Eef1b2, Eef2, Eef2a1, Eef2b, Eef3b, Eif3f, Eif3j1, Eno1, Enpp5, Epp41l2, Eprs, Erip44, Fat2, Fam20c, Fam234b, Fam3a, Fam3c, Fn1, Fucal, Fucal2, Fxr2, G3bp1, Gaa, Galns, Galnt14, Galnt2, Gapdh, Gba, Gg, Gcg, Gla, Glib1, Glig1, Glipr2, Gltrd1, Gm2a, Gnal, Gnaol, Gnas, Gnb1, Gnb2, Gng4, Gngptg, Gns, Gosr1, Got2, Gpi1, Gprn1, Haplh4, Hexa, Hexb, Hmgb2, Hnmp, Hs2st1, Hsp90ab1, Hspa13, Hspa5, Hspa9, Hspe1, Hsp1d3b, Impad1, Ins1, Ins2, Ipo5, Iqgap1, Kif23, Kif5b, Kpnb1, Lamp1, Lamp2, Lamtor1, Lamtor3, Lnpap, Lrrc59, Lsr, Man1b1, Man2b1, Mdh2, Mif, Mrpl41, Myh9, Myl12b, Naga, Naglu, Nap1l1, Napa, Nestn, Ndggl, Ndst1, Ndufc2, Neu1, Neurod1, Npm1, Nprx1, Nsf, Nucleb1, Nucleb2, Os9, P4hb, Pam, Pcsk1, Pcsk1n, Pcsk2, Pdia3, Pdia6, Plbd2, Pld3, Plod1, Plod3, Ptp2, Pipp1, Ppia, Ppp2r2a, Pprc1, Prdx4, Prikaca, Prikcsb, Psap, Psc, Psmc4, Psmid11, Ptpm, Ptpm2, Qsox1, Qsox2, Rab10, Rab11a, Rab14, Rab1a, Rab1b, Rab2a, Rab3, Rab3d, Rab3e, Rab3f, Rab3g, Rab3i, Rab3j, Rab3k, Rab3l, Rab3m, Rab3n, Rab3o, Rab3p, Rab3q, Rab3r, Rab3s, Rab3t, Rab3u, Rab3v, Rab3w, Rab3x, Rab3y, Rab3z, Rab4, Rab4a, Rab4b, Rab4c, Rab4d, Rab4e, Rab4f, Rab4g, Rab4h, Rab4i, Rab4j, Rab4k, Rab4l, Rab4m, Rab4n, Rab4o, Rab4p, Rab4q, Rab4r, Rab4s, Rab4t, Rab4u, Rab4v, Rab4w, Rab4x, Rab4y, Rab4z, Rab5, Rab5a, Rab5b, Rab5c, Rab5d, Rab5e, Rab5f, Rab5g, Rab5h, Rab5i, Rab5j, Rab5k, Rab5l, Rab5m, Rab5n, Rab5o, Rab5p, Rab5q, Rab5r, Rab5s, Rab5t, Rab5u, Rab5v, Rab5w, Rab5x, Rab5y, Rab5z, Rab6, Rab6a, Rab6b, Rab6c, Rab6d, Rab6e, Rab6f, Rab6g, Rab6h, Rab6i, Rab6j, Rab6k, Rab6l, Rab6m, Rab6n, Rab6o, Rab6p, Rab6q, Rab6r, Rab6s, Rab6t, Rab6u, Rab6v, Rab6w, Rab6x, Rab6y, Rab6z, Rab7, Rab7a, Rab7b, Rab7c, Rab7d, Rab7e, Rab7f, Rab7g, Rab7h, Rab7i, Rab7j, Rab7k, Rab7l, Rab7m, Rab7n, Rab7o, Rab7p, Rab7q, Rab7r, Rab7s, Rab7t, Rab7u, Rab7v, Rab7w, Rab7x, Rab7y, Rab7z, Rab8, Rab8a, Rab8b, Rab8c, Rab8d, Rab8e, Rab8f, Rab8g, Rab8h, Rab8i, Rab8j, Rab8k, Rab8l, Rab8m, Rab8n, Rab8o, Rab8p, Rab8q, Rab8r, Rab8s, Rab8t, Rab8u, Rab8v, Rab8w, Rab8x, Rab8y, Rab8z, Rab9, Rab9a, Rab9b, Rab9c, Rab9d, Rab9e, Rab9f, Rab9g, Rab9h, Rab9i, Rab9j, Rab9k, Rab9l, Rab9m, Rab9n, Rab9o, Rab9p, Rab9q, Rab9r, Rab9s, Rab9t, Rab9u, Rab9v, Rab9w, Rab9x, Rab9y, Rab9z, Rab10, Rab10a, Rab10b, Rab10c, Rab10d, Rab10e, Rab10f, Rab10g, Rab10h, Rab10i, Rab10j, Rab10k, Rab10l, Rab10m, Rab10n, Rab10o, Rab10p, Rab10q, Rab10r, Rab10s, Rab10t, Rab10u, Rab10v, Rab10w, Rab10x, Rab10y, Rab10z, Rab11, Rab11a, Rab11b, Rab11c, Rab11d, Rab11e, Rab11f, Rab11g, Rab11h, Rab11i, Rab11j, Rab11k, Rab11l, Rab11m, Rab11n, Rab11o, Rab11p, Rab11q, Rab11r, Rab11s, Rab11t, Rab11u, Rab11v, Rab11w, Rab11x, Rab11y, Rab11z, Rab12, Rab12a, Rab12b, Rab12c, Rab12d, Rab12e, Rab12f, Rab12g, Rab12h, Rab12i, Rab12j, Rab12k, Rab12l, Rab12m, Rab12n, Rab12o, Rab12p, Rab12q, Rab12r, Rab12s, Rab12t, Rab12u, Rab12v, Rab12w, Rab12x, Rab12y, Rab12z, Rab13, Rab13a, Rab13b, Rab13c, Rab13d, Rab13e, Rab13f, Rab13g, Rab13h, Rab13i, Rab13j, Rab13k, Rab13l, Rab13m, Rab13n, Rab13o, Rab13p, Rab13q, Rab13r, Rab13s, Rab13t, Rab13u, Rab13v, Rab13w, Rab13x, Rab13y, Rab13z, Rab14, Rab14a, Rab14b, Rab14c, Rab14d, Rab14e, Rab14f, Rab14g, Rab14h, Rab14i, Rab14j, Rab14k, Rab14l, Rab14m, Rab14n, Rab14o, Rab14p, Rab14q, Rab14r, Rab14s, Rab14t, Rab14u, Rab14v, Rab14w, Rab14x, Rab14y, Rab14z, Rab15, Rab15a, Rab15b, Rab15c, Rab15d, Rab15e, Rab15f, Rab15g, Rab15h, Rab15i, Rab15j, Rab15k, Rab15l, Rab15m, Rab15n, Rab15o, Rab15p, Rab15q, Rab15r, Rab15s, Rab15t, Rab15u, Rab15v, Rab15w, Rab15x, Rab15y, Rab15z, Rab16, Rab16a, Rab16b, Rab16c, Rab16d, Rab16e, Rab16f, Rab16g, Rab16h, Rab16i, Rab16j, Rab16k, Rab16l, Rab16m, Rab16n, Rab16o, Rab16p, Rab16q, Rab16r, Rab16s, Rab16t, Rab16u, Rab16v, Rab16w, Rab16x, Rab16y, Rab16z, Rab17, Rab17a, Rab17b, Rab17c, Rab17d, Rab17e, Rab17f, Rab17g, Rab17h, Rab17i, Rab17j, Rab17k, Rab17l, Rab17m, Rab17n, Rab17o, Rab17p, Rab17q, Rab17r, Rab17s, Rab17t, Rab17u, Rab17v, Rab17w, Rab17x, Rab17y, Rab17z, Rab18, Rab18a, Rab18b, Rab18c, Rab18d, Rab18e, Rab18f, Rab18g, Rab18h, Rab18i, Rab18j, Rab18k, Rab18l, Rab18m, Rab18n, Rab18o, Rab18p, Rab18q, Rab18r, Rab18s, Rab18t, Rab18u, Rab18v, Rab18w, Rab18x, Rab18y, Rab18z, Rab19, Rab19a, Rab19b, Rab19c, Rab19d, Rab19e, Rab19f, Rab19g, Rab19h, Rab19i, Rab19j, Rab19k, Rab19l, Rab19m, Rab19n, Rab19o, Rab19p, Rab19q, Rab19r, Rab19s, Rab19t, Rab19u, Rab19v, Rab19w, Rab19x, Rab19y, Rab19z, Rab20, Rab20a, Rab20b, Rab20c, Rab20d, Rab20e, Rab20f, Rab20g, Rab20h, Rab20i, Rab20j, Rab20k, Rab20l, Rab20m, Rab20n, Rab20o, Rab20p, Rab20q, Rab20r, Rab20s, Rab20t, Rab20u, Rab20v, Rab20w, Rab20x, Rab20y, Rab20z, Rab21, Rab21a, Rab21b, Rab21c, Rab21d, Rab21e, Rab21f, Rab21g, Rab21h, Rab21i, Rab21j, Rab21k, Rab21l, Rab21m, Rab21n, Rab21o, Rab21p, Rab21q, Rab21r, Rab21s, Rab21t, Rab21u, Rab21v, Rab21w, Rab21x, Rab21y, Rab21z, Rab22, Rab22a, Rab22b, Rab22c, Rab22d, Rab22e, Rab22f, Rab22g, Rab22h, Rab22i, Rab22j, Rab22k, Rab22l, Rab22m, Rab22n, Rab22o, Rab22p, Rab22q, Rab22r, Rab22s, Rab22t, Rab22u, Rab22v, Rab22w, Rab22x, Rab22y, Rab22z, Rab23, Rab23a, Rab23b, Rab23c, Rab23d, Rab23e, Rab23f, Rab23g, Rab23h, Rab23i, Rab23j, Rab23k, Rab23l, Rab23m, Rab23n, Rab23o, Rab23p, Rab23q, Rab23r, Rab23s, Rab23t, Rab23u, Rab23v, Rab23w, Rab23x, Rab23y, Rab23z, Rab24, Rab24a, Rab24b, Rab24c, Rab24d, Rab24e, Rab24f, Rab24g, Rab24h, Rab24i, Rab24j, Rab24k, Rab24l, Rab24m, Rab24n, Rab24o, Rab24p, Rab24q, Rab24r, Rab24s, Rab24t, Rab24u, Rab24v, Rab24w, Rab24x, Rab24y, Rab24z, Rab25, Rab25a, Rab25b, Rab25c, Rab25d, Rab25e, Rab25f, Rab25g, Rab25h, Rab25i, Rab25j, Rab25k, Rab25l, Rab25m, Rab25n, Rab25o, Rab25p, Rab25q, Rab25r, Rab25s, Rab25t, Rab25u, Rab25v, Rab25w, Rab25x, Rab25y, Rab25z, Rab26, Rab26a, Rab26b, Rab26c, Rab26d, Rab26e, Rab26f, Rab26g, Rab26h, Rab26i, Rab26j, Rab26k, Rab26l, Rab26m, Rab26n, Rab26o, Rab26p, Rab26q, Rab26r, Rab26s, Rab26t, Rab26u, Rab26v, Rab26w, Rab26x, Rab26y, Rab26z, Rab27, Rab27a, Rab27b, Rab27c, Rab27d, Rab27e, Rab27f, Rab27g, Rab27h, Rab27i, Rab27j, Rab27k, Rab27l, Rab27m, Rab27n, Rab27o, Rab27p, Rab27q, Rab27r, Rab27s, Rab27t, Rab27u, Rab27v, Rab27w, Rab27x, Rab27y, Rab27z, Rab28, Rab28a, Rab28b, Rab28c, Rab28d, Rab28e, Rab28f, Rab28g, Rab28h, Rab28i, Rab28j, Rab28k, Rab28l, Rab28m, Rab28n, Rab28o, Rab28p, Rab28q, Rab28r, Rab28s, Rab28t, Rab28u, Rab28v, Rab28w, Rab28x, Rab28y, Rab28z, Rab29, Rab29a, Rab29b, Rab29c, Rab29d, Rab29e, Rab29f, Rab29g, Rab29h, Rab29i, Rab29j, Rab29k, Rab29l, Rab29m, Rab29n, Rab29o, Rab29p, Rab29q, Rab29r, Rab29s, Rab29t, Rab29u, Rab29v, Rab29w, Rab29x, Rab29y, Rab29z, Rab30, Rab30a, Rab30b, Rab30c, Rab30d, Rab30e, Rab30f, Rab30g, Rab30h, Rab30i, Rab30j, Rab30k, Rab30l, Rab30m, Rab30n, Rab30o, Rab30p, Rab30q, Rab30r, Rab30s, Rab30t, Rab30u, Rab30v, Rab30w, Rab30x, Rab30y, Rab30z, Rab31, Rab31a, Rab31b, Rab31c, Rab31d, Rab31e, Rab31f, Rab31g, Rab31h, Rab31i, Rab31j, Rab31k, Rab31l, Rab31m, Rab31n, Rab31o, Rab31p, Rab31q, Rab31r, Rab31s, Rab31t, Rab31u, Rab31v, Rab31w, Rab31x, Rab31y, Rab31z, Rab32, Rab32a, Rab32b, Rab32c, Rab32d, Rab32e, Rab32f, Rab32g, Rab32h, Rab32i, Rab32j, Rab32k, Rab32l, Rab32m, Rab32n, Rab32o, Rab32p, Rab32q, Rab32r, Rab32s, Rab32t, Rab32u, Rab32v, Rab32w, Rab32x, Rab32y, Rab32z, Rab33, Rab33a, Rab33b, Rab33c, Rab33d, Rab33e, Rab33f, Rab33g, Rab33h, Rab33i, Rab33j, Rab33k, Rab33l, Rab33m, Rab33n, Rab33o, Rab33p, Rab33q, Rab33r, Rab33s, Rab33t, Rab33u, Rab33v, Rab33w, Rab33x, Rab33y, Rab33z, Rab34, Rab34a, Rab34b, Rab34c, Rab34d, Rab34e, Rab34f, Rab34g, Rab34h, Rab34i, Rab34j, Rab34k, Rab34l, Rab34m, Rab34n, Rab34o, Rab34p, Rab34q, Rab34r, Rab34s, Rab34t, Rab34u, Rab34v, Rab34w, Rab34x, Rab34y, Rab34z, Rab35, Rab35a, Rab35b, Rab35c, Rab35d, Rab35e, Rab35f, Rab35g, Rab35h, Rab35i, Rab35j, Rab35k, Rab35l, Rab35m, Rab35n, Rab35o, Rab35p, Rab35q, Rab35r, Rab35s, Rab35t, Rab35u, Rab35v, Rab35w, Rab35x, Rab35y, Rab35z, Rab36, Rab36a, Rab36b, Rab36c, Rab36d, Rab36e, Rab36f, Rab36g, Rab36h, Rab36i, Rab36j, Rab36k, Rab36l, Rab36m, Rab36n, Rab36o, Rab36p, Rab36q, Rab36r, Rab36s, Rab36t, Rab36u, Rab36v, Rab36w, Rab36x, Rab36y, Rab36z, Rab37, Rab37a, Rab37b, Rab37c, Rab37d, Rab37e, Rab37f, Rab37g, Rab37h, Rab37i, Rab37j, Rab37k, Rab37l, Rab37m, Rab37n, Rab37o, Rab37p, Rab37q, Rab37r, Rab37s, Rab37t, Rab37u, Rab37v, Rab37w, Rab37x, Rab37y, Rab37z, Rab38, Rab38a, Rab38b, Rab38c, Rab38d, Rab38e, Rab38f, Rab38g, Rab38h, Rab38i, Rab38j, Rab38k, Rab38l, Rab38m, Rab38n, Rab38o, Rab38p, Rab38q, Rab38r, Rab38s, Rab38t, Rab38u, Rab38v, Rab38w, Rab38x, Rab38y, Rab38z, Rab39, Rab39a, Rab39b, Rab39c, Rab39d, Rab39e, Rab39f, Rab39g, Rab39h, Rab39i, Rab39j, Rab39k, Rab39l, Rab39m, Rab39n, Rab39o, Rab39p, Rab39q, Rab39r, Rab39s, Rab39t, Rab39u, Rab39v, Rab39w, Rab39x, Rab39y, Rab39z, Rab40, Rab40a, Rab40b, Rab40c, Rab40d, Rab40e, Rab40f, Rab40g, Rab40h, Rab40i, Rab40j, Rab40k, Rab40l, Rab40m, Rab40n, Rab40o, Rab40p, Rab40q, Rab40r, Rab40s, Rab40t, Rab40u, Rab40v, Rab40w, Rab40x, Rab40y, Rab40z, Rab41, Rab41a, Rab41b, Rab41c, Rab41d, Rab41e, Rab41f, Rab41g, Rab41h, Rab41i, Rab41j, Rab41k, Rab41l, Rab41m, Rab41n, Rab41o, Rab41p, Rab41q, Rab41r, Rab41s, Rab41t, Rab41u, Rab41v, Rab41w, Rab41x, Rab41y, Rab41z, Rab42, Rab42a, Rab42b, Rab42c, Rab42d, Rab42e, Rab42f, Rab42g, Rab42h, Rab42i, Rab42j, Rab42k, Rab42l, Rab42m, Rab42n, Rab42o, Rab42p, Rab42q, Rab42r, Rab42s, Rab42t, Rab42u, Rab42v, Rab42w, Rab42x, Rab42y, Rab42z, Rab43, Rab43a, Rab43b, Rab43c, Rab43d, Rab43e, Rab43f, Rab43g, Rab43h, Rab43i, Rab43j, Rab43k, Rab43l, Rab43m, Rab43n, Rab43o, Rab43p, Rab43q, Rab43r, Rab43s, Rab43t, Rab43u, Rab43v, Rab43w, Rab43x, Rab43y, Rab43z, Rab44, Rab44a, Rab44b, Rab44c, Rab44d, Rab44e, Rab44f, Rab44g, Rab44h, Rab44i, Rab44j, Rab44k, Rab44l, Rab44m, Rab44n, Rab44o, Rab44p, Rab44q, Rab44r, Rab44s, Rab44t, Rab44u, Rab44v, Rab44w, Rab44x, Rab44y, Rab44z, Rab45, Rab45a, Rab45b, Rab45c, Rab45d, Rab45e, Rab45f, Rab45g, Rab45h, Rab45i, Rab45j, Rab45k, Rab45l, Rab45m, Rab45n, Rab45o, Rab45p, Rab45q, Rab45r, Rab45s, Rab45t, Rab45u, Rab45v, Rab45w, Rab45x, Rab45y, Rab45z, Rab46, Rab46a, Rab46b, Rab46c, Rab46d, Rab46e, Rab46f, Rab46g, Rab46h, Rab46i, Rab46j, Rab46k, Rab46l, Rab46m, Rab46n, Rab46o, Rab46p, Rab46q, Rab46r, Rab46s, Rab46t, Rab46u, Rab46v, Rab46w, Rab46x, Rab46y, Rab46z, Rab47, Rab47a, Rab47b, Rab47c, Rab47d, Rab47e, Rab47f, Rab47g, Rab47h, Rab47i, Rab47j, Rab47k, Rab47l, Rab47m, Rab47n, Rab47o, Rab47p, Rab47q, Rab47r, Rab47s, Rab47t, Rab47u, Rab47v, Rab47w, Rab47x, Rab47y, Rab47z, Rab48, Rab48a, Rab48b, Rab48c, Rab48d, Rab48e, Rab48f, Rab48g, Rab48h, Rab48i, Rab48j, Rab48k, Rab48l, Rab48m, Rab48n, Rab48o, Rab48p, Rab48q, Rab48r, Rab48s, Rab48t, Rab48u, Rab48v, Rab48w, Rab48x, Rab48y, Rab48z, Rab49, Rab49a, Rab49b, Rab49c, Rab49d, Rab49e, Rab49f, Rab49g, Rab49h, Rab49i, Rab49j, Rab49k, Rab49l, Rab49m, Rab49n, Rab49o, Rab49p, Rab49q, Rab49r, Rab49s, Rab49t, Rab49u, Rab49v, Rab49w, Rab49x, Rab49y, Rab49z, Rab50, Rab50a, Rab50b, Rab50c, Rab50d, Rab50e, Rab50f, Rab50g, Rab50h, Rab50i, Rab50j, Rab50k, Rab50l, Rab50m, Rab50n, Rab50o, Rab50p, Rab50q, Rab50r, Rab50s, Rab50t, Rab50u, Rab50v, Rab50w, Rab50x, Rab50y, Rab50z, Rab51, Rab51a, Rab51b, Rab51c, Rab51d, Rab51e, Rab51f, Rab51g, Rab51h, Rab51i, Rab51j, Rab51k, Rab51l, Rab51m, Rab51n, Rab51o, Rab51p, Rab51q, Rab51r, Rab51s, Rab51t, Rab51u, Rab51v, Rab51w, Rab51x, Rab51y, Rab51z, Rab52, Rab52a, Rab52b, Rab52c, Rab52d, Rab52e, Rab52f, Rab52g, Rab52h, Rab52i, Rab52j, Rab52k, Rab52l, Rab52m, Rab52n, Rab52o, Rab52p, Rab52q, Rab52r, Rab52s, Rab52t, Rab52u, Rab52v, Rab52w, Rab52x, Rab52y, Rab52z, Rab53, Rab53a, Rab53b, Rab53c, Rab53d, Rab53e, Rab53f, Rab53g, Rab53h, Rab53i, Rab53j, Rab53k, Rab53l, Rab53m, Rab53n, Rab53o, Rab53p, Rab53q, Rab53r, Rab53s, Rab53t, Rab53u, Rab53v, Rab53w, Rab53x, Rab53y, Rab53z, Rab54, Rab54a, Rab54b, Rab54c, Rab54d, Rab54e, Rab54f, Rab54g, Rab54h, Rab54i, Rab54j, Rab54k, Rab54l, Rab54m, Rab54n, Rab54o, Rab54p, Rab54q, Rab54r, Rab54s, Rab54t, Rab54u, Rab54v, Rab54w, Rab54x, Rab54y, Rab54z, Rab55, Rab55a, Rab55b, Rab55c, Rab55d, Rab55e, Rab55f, Rab55g, Rab55h, Rab55i, Rab55j, Rab55k, Rab55l, Rab55m, Rab55n, Rab55o, Rab55p, Rab55q, Rab55r, Rab55s, Rab55t, Rab55u, Rab55v, Rab55w, Rab55x, Rab55y, Rab55z, Rab56, Rab56a, Rab56b, Rab56c, Rab56d, Rab56e, Rab56f, Rab56g, Rab56h, Rab56i, Rab56j, Rab56k, Rab56l, Rab56m, Rab56n, Rab56o, Rab56p, Rab56q, Rab56r, Rab56s, Rab56t, Rab56u, Rab56v, Rab56w, Rab56x, Rab56y, Rab56z, Rab57, Rab57a, Rab57b, Rab57c, Rab57d, Rab57e, Rab57f, Rab57g, Rab57h, Rab57i, Rab57j, Rab57k, Rab57l, Rab57m, Rab57n, Rab57o, Rab57p, Rab57q, Rab57r, Rab57s, Rab57t, Rab57u, Rab57v, Rab57w, Rab57x, Rab57y, Rab57z, Rab58, Rab58a, Rab58b, Rab58c, Rab58d, Rab58e, Rab58f, Rab58g, Rab58h, Rab58i, Rab58j, Rab58k, Rab58l, Rab58m, Rab58n, Rab58o, Rab58p, Rab58q, Rab58r, Rab58s, Rab58t, Rab58u, Rab58v, Rab58w, Rab58x, Rab58y, Rab58z, Rab59, Rab59a, Rab59b, Rab59c, Rab59d, Rab59e, Rab59f, Rab59g, Rab59h, Rab59i, Rab59j, Rab59k, Rab59l, Rab59m, Rab59n, Rab59o, Rab59p, Rab59q, Rab59r, Rab59s, Rab59t, Rab59u, Rab59v, Rab59w, Rab59x, Rab59y, Rab59z, Rab60, Rab60a, Rab60b, Rab60c, Rab60d, Rab60e, Rab60f, Rab60g, Rab60h, Rab60i, Rab60j, Rab60k, Rab60l, Rab60m, Rab60n, Rab60o, Rab60p, Rab60q, Rab60r, Rab60s, Rab60t, Rab60u, Rab60v, Rab60w, Rab60x, Rab60y, Rab60z, Rab61, Rab61a, Rab61b, Rab61c, Rab61d, Rab61e, Rab61f, Rab61g, Rab61h, Rab61i, Rab61j, Rab61k, Rab61l, Rab61m, Rab61n, Rab61o, Rab61p, Rab61q, Rab61r, Rab61s, Rab61t, Rab61u, Rab61v, Rab61w, Rab61x, Rab61y, Rab61z, Rab62, Rab62a, Rab62b, Rab62c, Rab62d, Rab62e, Rab62f, Rab62g, Rab62h, Rab62i, Rab62j, Rab62k, Rab62l, Rab62m, Rab62n, Rab62o, Rab62p, Rab62q, Rab62r, Rab62s, Rab62t, Rab62u, Rab62v, Rab62w, Rab62x, Rab62y, Rab62z, Rab63, Rab63a, Rab63b, Rab63c, Rab63d, Rab63e, Rab63f, Rab63g, Rab63h, Rab63i, Rab63j, Rab63k, Rab63l, Rab63m, Rab63n, Rab63o, Rab63p, Rab63q, Rab63r, Rab63s, Rab63t, Rab63u, Rab63v, Rab63w, Rab63x, Rab63y, Rab63z, Rab64, Rab64a, Rab64b, Rab64c, Rab64d, Rab64e, Rab64f, Rab64g, Rab64h, Rab64i, Rab64j, Rab64k, Rab64l, Rab64m, Rab64n, Rab64o, Rab64p, Rab64q, Rab64r, Rab64s, Rab64t, Rab64u, Rab64v, Rab64w, Rab64x, Rab64y, Rab64z, Rab65, Rab65a, Rab65b, Rab65c, Rab65d, Rab65e, Rab65f, Rab65g, Rab65h, Rab65i, Rab65j, Rab65k, Rab65l, Rab65m, Rab65n, Rab65o, Rab65p, Rab65q, Rab65r, Rab65s, Rab65t, Rab65u, Rab65v, Rab65w, Rab65x, Rab65y, Rab65z, Rab66, Rab66a, Rab66b, Rab66c, Rab66d, Rab66e, Rab66f, Rab66g, Rab66h, Rab66i, Rab66j, Rab66k, Rab66l, Rab66m, Rab66n, Rab66o, Rab66p, Rab66q, Rab66r, Rab66s, Rab66t, Rab66u, Rab66v, Rab66w, Rab66x, Rab66y, Rab66z, Rab67, Rab67a, Rab67b, Rab67c, Rab67d, Rab67e, Rab67f, Rab67g, Rab67h, Rab67i, Rab67j, Rab67k, Rab67l, Rab67m, Rab67n, Rab67o, Rab67p, Rab67q, Rab67r, Rab67s, Rab67t, Rab67u, Rab67v, Rab67w, Rab67x, Rab67y, Rab67z, Rab68, Rab68a, Rab68b, Rab68c, Rab68d, Rab68e, Rab68f, Rab68g, Rab68h, Rab68i, Rab68j, Rab68k, Rab68l, Rab68m, Rab68n, Rab68o, Rab68p, Rab68q, Rab68r, Rab68s, Rab68t, Rab68u, Rab68v, Rab68w, Rab68x, Rab68y, Rab68z, Rab69, Rab69a, Rab69b, Rab69c, Rab69d, Rab69e, Rab69f, Rab69g, Rab69h, Rab69i, Rab69j, Rab69k, Rab69l, Rab69m, Rab69n, Rab69o, Rab69p, Rab69q, Rab69r, Rab69s, Rab69t, Rab69u, Rab69v, Rab69w, Rab69x, Rab69y, Rab69z, Rab70, Rab70a, Rab70b, Rab70c, Rab70d, Rab70e, Rab70f, Rab70g, Rab70h, Rab70i, Rab70j, Rab70k, Rab70l, Rab70m, Rab70n, Rab70o, Rab70p, Rab70q, Rab70r, Rab70s, Rab70t, Rab70u, Rab70v, Rab70w, Rab70x, Rab70y, Rab70z, Rab71, Rab71a, Rab71b, Rab71c, Rab71d, Rab71e, Rab71f, Rab71g, Rab71h, Rab71i, Rab71j, Rab71k, Rab71l, Rab71m, Rab71n, Rab71o, Rab71p, Rab71q, Rab71r, Rab71s, Rab71t, Rab71u, Rab71v, Rab71w, Rab71x, Rab71y, Rab71z, Rab72, Rab72a, Rab72b, Rab72c, Rab72d, Rab72e, Rab72f, Rab72g, Rab72h, Rab72i, Rab72j, Rab72k, Rab72l, Rab72m, Rab72n, Rab72o, Rab72p, Rab72q, Rab72r, Rab72s, Rab72t, Rab72u, Rab72v, Rab72w, Rab72x, Rab72y, Rab72z, Rab73, Rab73a, Rab73b, Rab73c, Rab73d, Rab73e, Rab73f, Rab73g, Rab73h, Rab73i, Rab73j, Rab73k, Rab73l, Rab73m, Rab73n, Rab73o, Rab73p, Rab73q, Rab73r, Rab73s, Rab73t, Rab73u, Rab73v, Rab73w, Rab73x, Rab73y, Rab73z, Rab74, Rab74a, Rab74b, Rab74c, Rab74d, Rab74e, Rab74f, Rab74g, Rab74h, Rab74i, Rab74j, Rab74k, Rab74l, Rab74m, Rab74n, Rab74o, Rab74p, Rab74q, Rab74r, Rab74s, Rab74t, Rab74u, Rab74v, Rab74w, Rab74x, Rab74y, Rab74z, Rab75, Rab75a, Rab75b, Rab75c, Rab75d, Rab75e, Rab75f, Rab75g, Rab75h, Rab75i, Rab75j, Rab75k, Rab75l, Rab75m, Rab75n, Rab75o, Rab75p, Rab75q, Rab75r, Rab75s, Rab75t, Rab75u, Rab75v, Rab75w, Rab75x, Rab75y, Rab75z, Rab76, Rab76a, Rab76b, Rab76c, Rab76d, Rab76e, Rab76f, Rab76g, Rab76h, Rab76i, Rab76j, Rab76k, Rab76l, Rab76m, Rab76n, Rab76o, Rab76p, Rab76q, Rab76r, Rab76s, Rab76t, Rab76u, Rab76v, Rab76w, Rab76x, Rab76y, Rab76z, Rab77, Rab77a, Rab77b, Rab77c, Rab77d, Rab77e, Rab77f, Rab77g, Rab77h, Rab77i, Rab77j, Rab77k, Rab77l, Rab77m, Rab77n, Rab77o, Rab77p, Rab77q, Rab77r, Rab77s, Rab77t, Rab77u, Rab77v, Rab77w, Rab77x, Rab77y, Rab77z, Rab78, Rab78a, Rab78b, Rab78c, Rab78d, Rab78e, Rab78f, Rab78g, Rab78h, Rab78i, Rab78j, Rab78k, Rab78l, Rab78m, Rab78n, Rab78o, Rab78p, Rab78q, Rab78r, Rab78s, Rab78t, Rab78u, Rab78v, Rab78w, Rab78x, Rab78y, Rab78z, Rab79, Rab79a, Rab79b, Rab79c, Rab79d, Rab79e, Rab79f, Rab79g, Rab79h, Rab79i, Rab79j, Rab79k, Rab79l, Rab79m, Rab79n, Rab79o, Rab79p, Rab79q, Rab79r, Rab79s, Rab79t, Rab79u, Rab79v, Rab79w, Rab79x, Rab79y, Rab79z, Rab80, Rab80a, Rab80b, Rab80c, Rab80d, Rab80e, Rab80f, Rab80g, Rab80h, Rab80i, Rab		

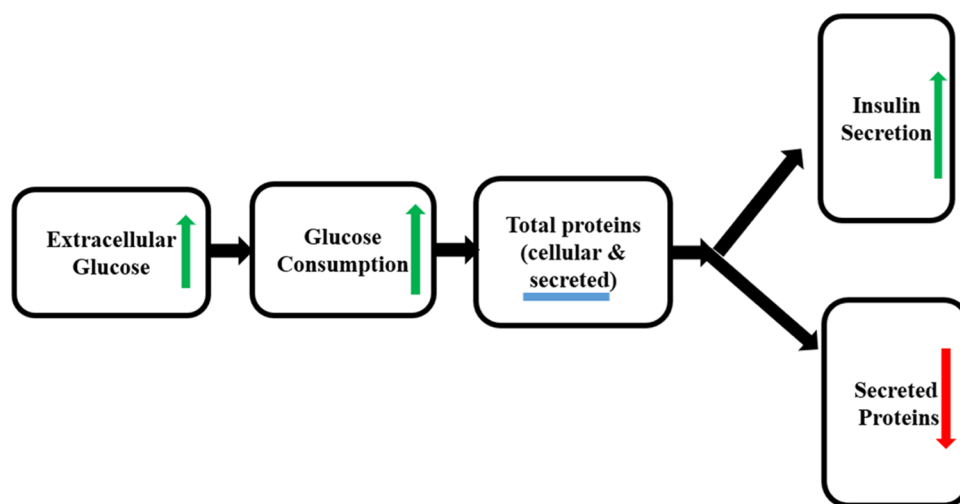


**Figure 4.** Conclusion summary: this shows a summarized conclusion where insulin is increasing at the cost of other extracellular secreted proteins.

the first clear indication of the fact that holistically viewing GSIS as a result of “Transcription + Translation + Secretory-Machinery/Mechanisms,” the onus may lay in post-transcriptional aspects substantially. To this end, it is important to note that the transcripts of insulin have also decreased at HyG concentration despite a 2-fold increase in insulin secretion at the secretion level, which strongly indicates a translational preference for insulin transcripts. It has also been analyzed previously in the literature that at high glucose concentrations, overall insulin mRNA remains the same, but a decrease in free cytoplasmic insulin mRNA and an increase in polysomal RNA were observed.<sup>27,28</sup> Cells favor insulin biosynthesis at the translational level at glucose stimulation over noninsulin protein, but which type of cellular proteins decrease or are compromised to favor insulin secretion has not been reported yet.<sup>27</sup> Insulin biosynthesis is mainly regulated at the translational level in cells at extracellular glucose stimulation, and the transcriptional product of preproinsulin is not directly proportional and does not reflect the translational product of insulin in pancreatic  $\beta$  cells.<sup>28–30</sup> This intriguing gap in knowledge presents an avenue for further investigation, potentially unraveling novel regulatory mechanisms governing insulin secretion by influencing or compromising other proteins. Some findings also support the important role of some insulin translational key players such as PABP (poly A binding protein) and PDI (protein disulfide isomerase). PDI overexpress at high glucose to increase insulin biosynthesis.<sup>31,32</sup> So, previous works support translation level regulation of insulin synthesis for a short period ( $\leq 1$  h).<sup>29</sup> Proteins, present in ISG, are essentially working for insulin granules biogenesis, maturation, and exocytosis at glucose stimulation.<sup>33</sup> Recent studies also find out the different granule populations related to different types of diabetes.<sup>34</sup> We have checked these ISG protein transcripts including insulin in the expression profile of our transcriptome studies. These proteins participate in the biogenesis and secretion of insulin.<sup>19,20</sup> Protein transcripts have been checked at HoG and HyG concentrations of glucose (shown in Figure 3c,d). Interestingly, transcripts of ISG related to extracellular and membrane/membrane-associated proteins do not change considerably.

In our studies, we have identified that cells decrease the transcripts of extracellular/secreted (nonmembrane) proteins

to favor insulin at high concentrations of glucose, as summarized in the flow diagram of the conclusion summary of Figure 4. This is also supported by the preference for secreted proteins due to the high metabolic cost for the processing of extracellular secreted proteins.<sup>13</sup> By the results of our findings, we can target future studies on the suppression of nonrequired and cost-expensive proteins to increase the secretion of insulin in the pancreatic  $\beta$  cells as a therapeutic tool to control blood glucose. This may be used to increase insulin secretion and maintain insulin levels in insulin-dependent diabetes.

Existing work indicates that cells prioritize insulin biosynthesis at the translational level. This emphasizes the significance of investigating both transcriptional and translational processes to gain a comprehensive understanding of insulin regulation and production. Our findings have specifically identified insulin, both at the transcriptional and translational levels, as well as other secreted proteins at the transcriptional level. The alterations detected in the cellular response are the result of the cellular reactions triggered by high glucose levels, which may impact various cellular processes, including those related to insulin and other proteins. This targeted analysis aims to establish potential correlations between insulin secretion and other extracellular secreted proteins. In addition to the above work, high glucose transport (from outside to inside the cells) is 100-fold higher than the intracellular phosphorylation of glucose.<sup>35</sup> This indicates that glucose not only works as a nutrient and an extracellular stimulator but also plays an important yet undiscovered role in modulating insulin secretion, especially considering the well-accepted glucose specificity in GSIS. In summary, glucose stimulates insulin biosynthesis and secretion by decreasing the extracellular secreted proteins.

**Clinical Implications.** On one hand, extrapolation of in vitro results, such as ours, to clinical implications is ambitious at best. On the other hand, a cellular level understanding and its clinical correlations are quite scarce despite more than half-a-century of recognizing the malaise of T1D. In this aspect, our findings create novel avenues for further research through some of the following clinical implications:

1. Clinically, GSIS results in an increased plasma insulin level that does not attain basal levels even after a few hours of postprandial time in healthy subjects (personal

communication by an anonymous reviewer). Thus, postprandial insulin levels tend to remain high even after plasma glucose levels are normalized in healthy subjects. While this does not have any cellular level understanding to date, our findings on the domination of translational + secretory machineries for insulin provide a direct connection. Post-induction of insulin transcription by high glucose levels and enhanced operations of translational + secretory machineries for insulin secretion (while reducing transcription of other secretory proteins) may explain the above observations in healthy subjects.

2. The development of a condition like T1D is attributed to the incapacity to generate and/or release insulin, likely resulting from the immune-driven destruction of pancreatic beta cells. However, our results indicate that hyperinsulinemia may also contribute to the development of T1D. Investment of excessive cellular energy/resources for enhancing secretory machinery specifically for insulin compared to other secretory proteins may exhaust the ability of beta cells to sustain their “regular” metabolism thereby, resulting in eventual destruction.
3. In Type 2 diabetes (T2D), glucose-consuming cells become insensitive to insulin. Consequently, at high glucose concentrations, beta cells increase their insulin secretion to the highest levels, resulting in hyperinsulinemia. Over time, again this chronic hyperinsulinemia may exert significant stress on pancreatic beta cells, potentially causing their “exhaustion” as above. Such beta cell exhaustion may ultimately contribute to the development of T1D, establishing an interplay between T1D and T2D. A similar concept may apply for utilization of insulin mimetics and antagonists secreted by pancreatic beta cells—the chronic hyperinsulinemia eventually lowers even transcriptional ability, in addition to secretion of whatever transcription takes place, of non-insulin secretory proteins.

## ■ CONCLUSIONS: IS THERE A LAW OF CONSERVATION OF SECRETED PROTEINS IN CELL BIOLOGY?

Laws and axioms with well-defined assumptions are central to mathematics, physics, and chemistry. The science of biology, however, is yet to benefit from the general acceptance of even a single universally applicable tenet despite some recent discoveries.<sup>36–38</sup> Arguably, the only consensus definition in biological sciences is that of a cell as a unit of life. Even the unparalleled discovery of the central dogma,<sup>39</sup> earlier believed to be universal, does not apply to certain aspects of biological replication.<sup>18</sup> On the one hand, a case-by-case assessment of phenomena renders biological sciences relatively empirical. On the other hand, continuing challenges associated with the discovery of exception-free universal features/signatures in systems are a major source of excitement in biological research. In spite of the above, several biotechnological advances continue to be fueled by explicit experimental characterization of living cells as chemically reacting species,<sup>40</sup> especially while scaling up bioreactions at industrial levels. Additionally, energetic constraints on cell sizes, cellular metabolism,<sup>41</sup> and synthesis of cellular organelles<sup>42</sup> have allowed physiochemical insights into operational limits for living cells. Even the physical process of protein folding has been shown to be

dependent on stoichiometric limits of amino acid constituents in primary sequences.<sup>36,38,43,44</sup>

In this work, we report a serendipitous discovery of another such operational limit in living cells. While working with “Mouse INSulinoma 6” (MIN6) cell lines as model systems toward understanding glucose-stimulated insulin secretion relevant to T1D, we have discovered a conservation mechanism in the secretory system; this may be applicable to all living cells. We report that total secretory proteins are maintained in a specific pool, which is kept constant through the exercise of transcriptional, translational, and intracellular trafficking control. The eventual release of specific proteins, triggered by external signals, results from the intricate interplay of secretory pathways and cascading cellular signals. It is noteworthy that secreted proteins impose the most significant energy demands on cells during their processing compared with other proteins. Furthermore, the additional task of correctly packaging these proteins within the cell for eventual release can place substantial demands on cells, potentially interfering with the synthesis and production of other proteins. Our research has revealed a noteworthy phenomenon: cells downregulate the transcripts of extracellular/secreted (non-membrane) proteins in favor of insulin when exposed to high glucose concentrations. We present a novel discovery: heightened insulin secretion comes at the expense of other secretory proteins while leaving other cellular proteins unaffected. Our findings unveil a compensatory trade-off involving other secretory proteins to facilitate enhanced glucose-stimulated insulin secretion (GSIS). This compensatory mechanism operates across three levels: transcriptional, translational, and the preparation of secretory vesicles (insulin granules). This intricate regulation highlights the complexity arising from GSIS and its profound effect on cellular secretory pathways. Our results not only provide cellular insights into the insulin secretion mechanisms but also indicate the unraveling of a conservatory nature of cellular secretions, which may be a general feature in cell biology.

## ■ MATERIALS AND METHODS

**Chemicals.** Fetal bovine serum (FBS), Dulbecco modified Eagle’s medium (DMEM), Pen–Strep, and trypsin–EDTA were obtained from Gibco. A Rat/Mouse (EZRMI-13K) Insulin enzyme-linked immunosorbent assay (ELISA) kit, ethanol, and monosodium phosphate ( $\text{NaH}_2\text{PO}_4$ ) were purchased from Merck. Glucose, calcium chloride ( $\text{CaCl}_2$ ), magnesium chloride ( $\text{MgCl}_2$ ), HEPES, potassium chloride (KCl), monopotassium phosphate ( $\text{KH}_2\text{PO}_4$ ), dipotassium phosphate ( $\text{K}_2\text{HPO}_4$ ), sodium chloride (NaCl), sodium bicarbonate ( $\text{NaHCO}_3$ ), 2-propanol, formaldehyde, BSA, and the Bradford assay were purchased from HiMedia, India. Glucose oxidase, horseradish peroxidase, 4-aminoantipyrine *N*-ethyl-*N*-sulfopropyl-*M*-toluidine, chloroform, and didium phosphate ( $\text{Na}_2\text{HPO}_4$ ) were purchased from Sigma, India. TRIzol was purchased for Ambion Life Technology, U.S.A.

**Cell Maintenance.** MIN6 cells were purchased from NCCS (National Center for Cell Science, Pune) and maintained in DMEM, 25 mM glucose, and 10% FBS with 1% Pen–Strep at 37 °C and 5%  $\text{CO}_2$ . Media was changed every second day to maintain healthy cells and split when required, according to the literature.<sup>45</sup> Experimental studies were performed with cell passages below 30. RAW264.7 cells were used as negative controls and maintained in the same media.



### MIN6-Glucose-Stimulated Insulin Secretion (GSIS).

Cells at a density of  $10 \times 10^5$  cells per well were seeded in a 6-well plate and used for the experiment after getting 75% confluency. The cells were washed with Krebs Ringer Bicarbonate Buffer (119 mM NaCl, 4.7 mM KCl, 1.2 mM  $MgSO_4$ , 2.5 mM  $CaCl_2$ ,  $KH_2PO_4$ , 25 mM  $NaHCO_3$ , and 10 mM HEPES with 0.1% BSA at pH 7.4) without glucose. KRBH buffer was supplemented with 1 mg/mL (0.1%) BSA to provide stabilization for the cells during the 1 h experimental incubation period. The cells were equilibrated at the hypoglycemic condition with KRBH 2.8 mM glucose for 0.5 h, and then glucose stimulation was given with 0, 2.8, 5.6, 8.3, 16.7, and 25 mM glucose in KRBH for 1 h at 37 °C and 5%  $CO_2$  as per protocol.<sup>46</sup> After 1 h incubation, the supernatant was removed, centrifuged at 2500 rpm for 5 min, and stored at -20 °C for estimation of insulin by the ELISA kit, EZRMI-13K Merck. Secreted insulin was normalized by total cellular protein estimated by the Bradford assay with BSA as a standard, and each treatment was performed in triplicate.

**Glucose Estimation.** From the above experiments, the removed supernatant contained residual glucose after glucose stimulation, which was used for glucose estimation, followed by the oxidase/peroxidase assay.<sup>46</sup> Glucose estimation was done in a total of 200  $\mu$ L of volume by taking 10 mM 4-aminoantipyrine, 10 mM *N*-ethyl-*N*-sulfo-propyl-*M*-toluidine with 0.16 U/mL horseradish peroxidase enzyme, and glucose sample in 80 mM sodium phosphate buffer at pH 6.0. Glucose oxidase (2.7 U/mL) was added at last to initiate the reaction. A standard curve was prepared from 0 to 45 mM glucose and afterward incubated for 45 min, and absorbance was checked at 550 nm by a Thermo Scientific Multiskan GO spectrophotometer.

**RNA Isolation.** Cells at a density of  $10 \times 10^5$  cells per well were seeded in a 6-well plate and used for the experiment after getting 75% confluency. The cells were equilibrated at 2.8 mM glucose for 0.5 h and then stimulated at 2.8 HoG and 25 mM HyG of glucose for 1 h in KRBH buffer. RNA was isolated, followed by TRIzol according to the manufacturer's protocol. We treated the cells with 1 mL of TRIzol and homogenized the cell pellet two to three times. Next, we added 0.2 mL of chloroform and incubated for 5 min on ice; now, we inverted the mix 10 times before incubating again for 2–3 min on ice. The sample was centrifuged in microcentrifuge tubes at 14,000 rpm for 15 min at 4 °C. After centrifugation, three layers were formed. The aqueous layer containing RNA was transferred to a new tube, and 0.5 mL of 2-propanol was added. The mix was inverted 10 times and incubated for 10 min at -20 °C. Now centrifuged at 14,000 rpm for 15 min, total RNA got pellet down. Next, we discarded the supernatant and added 1 mL of 75% ethanol. After that, the sample was air-dried, dissolved in RNase-free water, and stored at -80 °C for RNA sequencing studies.

**Transcriptome Studies.** Transcriptome studies were done by Agrigenome Lab Private Limited, Kerala, India. The quality and quantity of isolated RNA were checked using an Agilent TapeStation 2200 and a Qubit 3.0 fluorimeter. After preparation of the sample library, the quality of the library was checked using the Agilent TapeStation 2200 and quantified using the Qubit 3.0 fluorimeter, and the validated libraries were sequenced on an Illumina HiSeq X10 Platform for  $2 \times 150$  bp read length with a read depth of 50 million reads. Mapping to a reference genome is a crucial factor. Here, mapping was done on Hisat2 by taking reference genome

GRCm38 of *Mus musculus*. Gene expression analysis was done by using cuffdiff in the form of Fragments Per Kilobase of transcript per Million mapped reads (FPKM), whereas gene annotation was done with the help of uniprot. Transcriptome data were submitted to the database repositories of NCBI-GEO (National Center for Biotechnology Information—Gene Expression Omnibus) with an assigned accession number record of GSE226652. The entire differential gene expression analysis study can be viewed through the link: <https://www.ncbi.nlm.nih.gov/geo/query/acc.cgi?acc=GSE226652>.

**Data Filtration.** A total of 55,467 genes were given in transcriptome data, where 14,427 genes were segregated as successfully expressed after applying the filter “Ok” on the ‘status’ of the gene. Next, we separated 11,741 total proteins (TotPs) by applying filter “Protein-coding” on the ‘gene type’ from the successfully expressed genes. Afterward, we applied a filter “Extracellular” on the ‘cellular component,’ where we found 630 extracellular genes (membrane and nonmembrane proteins) from total protein. Next, we separated 320 membrane proteins by applying a filter “Membrane” again on the ‘cellular component,’ and the remaining 310 were nonmembrane proteins from 630 extracellular genes. We extracted 11,431 cellular protein transcripts from 11,741 total protein transcripts by deducting the 310 extracellular proteins (nonmembrane). We also filtered again from 11,741 proteins by applying the filter “Secret” (for words secreted, secretory, and secrete) on the ‘cellular component’ and separated 84 secretory proteins. In these proteins, a total of 30 (17 nonmembrane and 13 membranes) are a subset of the 630 extracellular proteins.

Proteins from 406 insulin secretory granules (ISGs) mentioned in the literature were checked and are tabulated in Supporting Table 3.<sup>22–25</sup> After removing common proteins from the superset of Supporting Table 3, 328 ISG proteins were identified and are tabulated in Table 1. A total of 296 ISGs were identified and have been checked as successfully expressed in our transcriptome data termed as detected (D). For genes that were not successfully expressed with ok status but had a reading, a total of 19 ISGs were termed as not detected (ND), and for those that were not present in our data, a total of 13 ISGs were shown as not present (NP), as mentioned in Table 1. Transcripts of these 296 ISG proteins were analyzed with and without insulin. Transcripts of ISG proteins were filtered after applying filters (29 “Extracellular,” 176 “Membrane” (membrane-associated), and rest as others) on ‘cellular component’ from a total of 296 ISG proteins, as shown in Figure 3a. Next, we identified ISG proteins from the literature, which was based on protein correlation profiling.<sup>25</sup> Here, 76 proteins were successfully expressed out of 81 proteins. The flow diagram in Figure 3b shows 76 successfully expressed proteins out of a total of 81. Transcripts of ISG proteins were filtered after applying filters (10 “Extracellular,” 59 “Membrane”(membrane-associated), and the rest are named as others) from a total of 76 ISG proteins, as shown in Figure 3b. **Note:** Filters that we have applied in this methodology were written in double (“”) inverted commas, and on which filters were applied were written in single (“”) inverted commas.

**Data Analysis.** Generally, transcriptome results are analyzed and presented in terms of Fragments Per Kilobase of transcript per Million mapped reads (FPKM). However, it was recently suggested that Transcripts Per Million (TPM) may be a more accurate way to compare transcriptomes across

samples.<sup>47</sup> So, we have checked our data in both ways. Both of the calculations give the same conclusion of the results. So, we have analyzed our results in both ways and TPM as well as values obtained by normalizing w.r.t. “ $\sum(\text{FPKM})$ ” and “ $\sum(\text{TPM})$ .” Conversion of TPM was done by using eq 1.

$$\text{TPM} = 10^6 \times \frac{\text{FPKM}}{\sum(\text{FPKM})} \quad (1)$$

Here, the transcript of proteins such as “Extracellular” is taken in the form of  $\sum\text{FPKM}$  and  $\sum\text{TPM}$ . Here, the results are calculated in the form of percentages at 2.8 and 25 mM glucose of total protein-coding transcripts by using eqs 2 and 3. Next, we calculated the % difference at 25 mM glucose for 2.8 mM glucose using eq 4. All data were normalized by 11,739 total proteins without insulin.

$$\text{initial (at 2.8 mM)} = \frac{\text{POI (2.8)}}{\text{TotP (2.8)}} \times 100 \quad (2)$$

$$\text{final (at 25 mM)} = \frac{\text{POI (25)}}{\text{TotP (25)}} \times 100 \quad (3)$$

$$\% \text{ diff at 25 M of glucose} = \frac{\text{final} - \text{initial}}{\text{initial}} \times 100 \quad (4)$$

POI = protein of interest

TotP = total protein.

**Statistical Analysis.** The results were represented as mean  $\pm$  standard deviation by using Microsoft Excel (2016). Statistical significance was checked by using Student's *t*-test on Microsoft Excel (2016). The results were considered statistically significant with *p* values <0.05.

## ■ ASSOCIATED CONTENT

### SI Supporting Information

The Supporting Information is available free of charge at <https://pubs.acs.org/doi/10.1021/acsomega.3c06058>.

Insulin secretion per mg of cellular protein; supernatant protein per mg of cellular protein; fraction of insulin secretion with supernatant protein; glucose consumption in moles per cell at different extracellular glucose; amount of supernatant protein in milligrams per cell; comparing transcript results with non-normalized values for Figure 2c; isoform analysis; transcripts values of Figure 2c in the form of TPM and FPKM; transcripts values of isoforms in the form of TPM and FPKM; ISG proteins from the literature; transcripts values of Figure 3c in the form of TPM and FPKM; and transcripts values of Figure 3d in the form of TPM and FPKM (PDF)

## ■ AUTHOR INFORMATION

### Corresponding Author

Aditya Mittal – Kusuma School of Biological Sciences, Indian Institute of Technology Delhi (IIT Delhi), New Delhi 110016, India; Supercomputing Facility for Bioinformatics and Computational Biology (SCFBio), IIT Delhi, New Delhi 110016, India; [orcid.org/0000-0002-4030-0951](https://orcid.org/0000-0002-4030-0951); Email: [amittal@bioschool.iitd.ac.in](mailto:amittal@bioschool.iitd.ac.in)

### Author

Firdos – Kusuma School of Biological Sciences, Indian Institute of Technology Delhi (IIT Delhi), New Delhi 110016, India

Complete contact information is available at: <https://pubs.acs.org/10.1021/acsomega.3c06058>

## Notes

The authors declare no competing financial interest.

## ■ ACKNOWLEDGMENTS

Firdos is grateful to the Council of Scientific and Industrial Research (CSIR), Govt. of India, for fellowship support. A.M. is grateful to (a) Siddhant Mittal for sharing clinical manifestations of Type 1 diabetes based on personal observations and (b) three (out of at least five) anonymous reviewers for highlighting the possible clinical relevance of our findings to not only Type 1 Diabetes but also the development of Type 1 Diabetes in Type 2 Diabetics. In fact, the brief section titled “Clinical Implications” was included at behest of the reviewers in the manuscript. A.M. is also grateful to Shweta Mittal and C. S. Dey for informal discussions that encouraged him to initiate research on cellular aspects related to Type 1 diabetes.

## ■ ABBREVIATIONS

GSIS: glucose-stimulated insulin secretion; T1D: type 1 diabetes; EGC: extracellular glucose concentrations; MIN6: mouse insulinoma 6; eIS: enhanced insulin secretion; DM: diabetes mellitus; ISGs: insulin secretory granules; HoG: hypoglycemic; HyG: hyperglycemic; FPKM: fragments per kilobase of transcript per million mapped reads; TPM: transcript per million

## ■ REFERENCES

- (1) Achenbach, P.; Bonifacio, E.; Koczwara, K.; Ziegler, A.-G. Natural History of Type 1 Diabetes. *Diabetes* **2005**, *54* (suppl\_2), S25–S31.
- (2) Gale, E. A. M. The Discovery of Type 1 Diabetes. *Diabetes* **2001**, *50* (2), 217–226.
- (3) Daneman, D. Type 1 diabetes. *Lancet* **2006**, *367* (9513), 847–858.
- (4) Home, Resources; diabetes, L. with; Acknowledgement; FAQs; Contact; Policy, P. IDF Diabetes Atlas 2021 | IDF Diabetes Atlas. IDF Diabetes Atlas. <https://diabetesatlas.org/atlas/tenth-edition/>.
- (5) Kollipara, S. Comorbidities associated with type 1 diabetes. *NASN School nurse* **2010**, *25* (1), 19–21.
- (6) Institute for Quality and Efficiency in Health Care. Hyperglycemia and Hypoglycemia in Type 1 Diabetes. <https://www.ncbi.nlm.nih.gov/books/NBK279340/>. (Accessed June 10, 2023).
- (7) Ceriello, A.; Monnier, L.; Owens, D. Glycaemic variability in diabetes: clinical and therapeutic implications. *Lancet Diabetes Endocrinol.* **2019**, *7* (3), 221–230.
- (8) Wintergerst, K. A.; Buckingham, B.; Gandrud, L.; Wong, B. J.; Kache, S.; Wilson, D. M. Association of hypoglycemia, hyperglycemia, and glucose variability with morbidity and death in the pediatric intensive care unit. *Pediatrics* **2006**, *118* (1), 173–179.
- (9) Miyazaki, J.; Araki, K.; Yamato, E.; Ikegami, H.; Asano, T.; Shibasaki, Y.; Oka, Y.; Yamamura, K. Establishment of a pancreatic  $\beta$  cell line that retains glucose-inducible insulin secretion: Special reference to expression of glucose transporter isoforms. *Endocrinology* **1990**, *127* (1), 126–132.
- (10) Ishihara, H.; Asano, T.; Tsukuda, K.; Katagiri, H.; Inukai, K.; Anai, M.; Kikuchi, M.; Yazaki, Y.; Miyazaki, J.-I.; Oka, Y. Pancreatic Beta Cell Line MIN6 Exhibits Characteristics of Glucose Metabolism and Glucose-Stimulated Insulin Secretion Similar to Those of Normal Islets. *Diabetologia* **1993**, *36* (11), 1139–1145.
- (11) Uhlén, M.; Fagerberg, L.; Hallström, B. M.; Lindskog, C.; Oksvold, P.; Mardinoglu, A.; Sivertsson, A.; Kampf, C.; Sjostedt, E.; Asplund, A.; Olsson, I.; Edlund, K.; Lundberg, E.; Navani, S.;

- Szigyarto, C. A.-K.; Odeberg, J.; Djureinovic, D.; Takanen, J. O.; Hober, S.; Alm, T.; et al. Tissue-based map of the human proteome. *Science* **2015**, *347* (6220), No. 1260419.
- (12) Farhan, H.; Rabouille, C. Signalling to and from the secretory pathway. *J. Cell Sci.* **2011**, *124* (2), 171–180.
- (13) Gutierrez, J. M.; Feizi, A.; Li, S.; Kallehauge, T. B.; Hefzi, H.; Grav, L. M.; Ley, D.; Hizal, D. B.; Betenbaugh, M. J.; Voldborg, B.; Kildegaard, H. F.; Lee, G. M.; Palsson, B. O.; Nielsen, J.; Lewis, N. E. Genome-scale reconstructions of the mammalian secretory pathway predict metabolic costs and limitations of protein secretion. *Nat. Commun.* **2020**, *11* (1), No. 68.
- (14) Detimary, P.; Dejonghe, S.; Ling, Z.; Pipeleers, D.; Schuit, F.; Henquin, J.-C. The changes in adenine nucleotides measured in glucose-stimulated rodent islets occur in  $\beta$  cells but not in  $\alpha$  cells and are also observed in human islets. *J. Biol. Chem.* **1998**, *273* (51), 33905–33908.
- (15) Detimary, P.; Jonas, J. C.; Henquin, J. C. Possible links between glucose-induced changes in the energy state of pancreatic B cells and insulin release: Unmasking by decreasing a stable pool of adenine nucleotides in mouse islets. *J. Clin. Invest.* **1995**, *96* (4), 1738–1745.
- (16) Sakamoto, S.; Miyaji, T.; Hiasa, M.; Ichikawa, R.; Uematsu, A.; Iwatsuki, K.; Shibata, A.; Uneyama, H.; Takayanagi, R.; Yamamoto, A.; Omote, H.; Nomura, M.; Moriyama, Y. Impairment of vesicular ATP release affects glucose metabolism and increases insulin sensitivity. *Sci. Rep.* **2014**, *4* (1), No. 6689.
- (17) Duvoor, C.; Dendi, V. S.; Marco, A.; Shekhawat, N. S.; Chada, A.; Ravilla, R.; Musham, C. K.; Mirza, W.; Chaudhury, A. Commentary: ATP: The crucial component of secretory vesicles: Accelerated ATP/insulin exocytosis and prediabetes. *Front. Physiol.* **2017**, *8*, No. 53, DOI: 10.3389/fphys.2017.00053.
- (18) Mittal, A.; Chauhan, A. Aspects of biological replication and evolution independent of the central dogma: Insights from protein-free vesicular transformations and protein-mediated membrane remodeling. *J. Membr. Biol.* **2022**, *255* (2–3), 185–209.
- (19) Germanos, M.; Gao, A.; Taper, M.; Yau, B.; Kebede, M. A. Inside the Insulin Secretory Granule. *Metabolites* **2021**, *11*, No. 515.
- (20) Suckale, J.; Solimena, M. The insulin secretory granule as a signaling hub. *Trends Endocrinol. Metab.* **2010**, *21* (10), 599–609.
- (21) Hutton, J. C.; Penn, E. J.; Peshavaria, M. Isolation and characterisation of insulin secretory granules from a rat islet cell tumour. *Diabetologia* **1982**, *23* (4), 365–373.
- (22) Brunner, Y.; Couté, Y.; Iezzi, M.; Foti, M.; Fukuda, M.; Hochstrasser, D. F.; Wollheim, C. B.; Sanchez, J.-C. Proteomics analysis of insulin secretory granules. *Mol. Cell. Proteomics* **2007**, *6* (6), 1007–1017.
- (23) Hickey, A. J. R.; Bradley, J. W. I.; Skea, G. L.; Middleditch, M. J.; Buchanan, C. M.; Phillips, A. R. J.; Cooper, G. J. S. Proteins associated with immunopurified granules from a model pancreatic islet  $\beta$ -Cell system: Proteomic snapshot of an endocrine secretory granule. *J. Proteome Res.* **2009**, *8* (1), 178–186.
- (24) Schwartz, D.; Brunner, Y.; Couté, Y.; Foti, M.; Wollheim, C. B.; Sanchez, J.-C. Improved characterization of the insulin secretory granule proteomes. *J. Proteomics* **2012**, *75* (15), 4620–4631.
- (25) Li, M.; Du, W.; Zhou, M.; Zheng, L.; Song, E.; Hou, J. Proteomic analysis of insulin secretory granules in INS-1 cells by protein correlation profiling. *Biophys. Rep.* **2018**, *4* (6), 329–338.
- (26) Norris, N.; Yau, B.; Kebede, M. A. Isolation and proteomics of the insulin secretory granule. *Metabolites* **2021**, *11* (5), No. 288.
- (27) Itoh, N.; Okamoto, H. Translational Control of Proinsulin Synthesis by Glucose. *Nature* **1980**, *283* (5742), 100–102.
- (28) Welsh, M. J.; Scherberg, N. H.; Gilmore, R. S.; Steiner, D. F. Translational Control of Insulin Biosynthesis. Evidence for Regulation of Elongation, Initiation and Signal-Recognition-Particle-Mediated Translational Arrest by Glucose. *Biochem. J.* **1986**, *235* (2), 459–467.
- (29) Wicksteed, B.; Alarcon, C.; Briaud, I.; Lingohr, M. K.; Rhodes, C. J. Glucose-Induced Translational Control of Proinsulin Biosynthesis Is Proportional to Preproinsulin mRNA Levels in Islet  $\beta$ -Cells but Not Regulated via a Positive Feedback of Secreted Insulin. *J. Biol. Chem.* **2003**, *278* (43), 42080–42090.
- (30) Evans-Molina, C.; Garmey, J. C.; Ketchum, R.; Brayman, K. L.; Deng, S.; Mirmira, R. G. Glucose regulation of insulin gene transcription and pre-mRNA processing in human islets. *Diabetes* **2007**, *56* (3), 827–835.
- (31) Kulkarni, S. D.; Muralidharan, B.; Panda, A. C.; Bakthavachalu, B.; Vindu, A.; Seshadri, V. Glucose-stimulated translation regulation of insulin by the 5' UTR-binding proteins. *J. Biol. Chem.* **2011**, *286* (16), 14146–14156.
- (32) Pandey, P. R.; Sarwade, R. D.; Khaliq, A.; Seshadri, V. Interaction of HuDA and PABP at 5'UTR of Mouse Insulin2 Regulates Insulin Biosynthesis. *PLoS One* **2018**, *13* (3), No. e0194482.
- (33) Omar-Hmeadi, M.; Idevall-Hagren, O. Insulin Granule Biogenesis and Exocytosis. *Cell. Mol. Life Sci.* **2021**, *78*, 1957–1970.
- (34) Kreutzberger, A. J. B.; Kiessling, V.; Doyle, C. A.; et al. Distinct insulin granule subpopulations implicated in the secretory pathology of diabetes types 1 and 2. *eLife* **2020**, *9*, No. e62506.
- (35) Tal, M.; Liang, Y.; Najafi, H.; Lodish, H. F.; Matschinsky, F. M. Expression and Function of GLUT-1 and GLUT-2 Glucose Transporter Isoforms in Cells of Cultured Rat Pancreatic Islets. *J. Biol. Chem.* **1992**, *267* (24), 17241–17247.
- (36) Mittal, A.; Jayaram, B.; Shenoy, S.; Bawa, T. S. A stoichiometry driven universal spatial organization of backbones of folded proteins: Are there Chargaff's rules for protein folding? *J. Biomol. Struct. Dyn.* **2010**, *28* (2), 133–142.
- (37) Mittal, A.; Jayaram, B. Backbones of Folded Proteins Reveal Novel Invariant Amino Acid Neighborhoods. *J. Biomol. Struct. Dyn.* **2011**, *28* (4), 443–454.
- (38) Mittal, A.; Jayaram, B. The Newest View on Protein Folding: Stoichiometric and Spatial Unity in Structural and Functional Diversity. *J. Biomol. Struct. Dyn.* **2011**, *28* (4), 669–674.
- (39) Crick, F. Central Dogma of Molecular Biology. *Nature* **1970**, *227* (5258), 561–563.
- (40) Naresh, M.; Das, S.; Mishra, P.; Mittal, A. The Chemical Formula of a Magnetotactic Bacterium. *Biotechnol. Bioeng.* **2012**, *109* (5), 1205–1216.
- (41) Szenk, M.; Dill, K. A.; de Graff, A. M. R. Why Do Fast-Growing Bacteria Enter Overflow Metabolism? Testing the Membrane Real Estate Hypothesis. *Cell Syst.* **2017**, *5* (2), 95–104.
- (42) Naresh, M.; Hasija, V.; Sharma, M.; Mittal, A. Synthesis of cellular organelles containing nano-magnets stunts growth of magnetotactic bacteria. *J. Nanosci. Nanotechnol.* **2010**, *10* (7), 4135–4144.
- (43) Mittal, A.; Changani, A. M.; Taparia, S.; Goel, D.; Parihar, A.; Singh, I. Structural Disorder Originates beyond Narrow Stoichiometric Margins of Amino Acids in Naturally Occurring Folded Proteins. *J. Biomol. Struct. Dyn.* **2021**, *39* (7), 2364–2375.
- (44) Mittal, A.; Changani, A. M.; Taparia, S. What Limits the Primary Sequence Space of Natural Proteins? *J. Biomol. Struct. Dyn.* **2020**, *38* (15), 4579–4583.
- (45) O'Driscoll, L.; Gammell, P.; Clynes, M. Mechanisms Associated with Loss of Glucose Responsiveness in Beta Cells. *Transplant. Proc.* **2004**, *36* (4), 1159–1162.
- (46) Blake, D. A.; McLean, N. V. A Colorimetric Assay for the Measurement of D-Glucose Consumption by Cultured Cells. *Anal. Biochem.* **1989**, *177* (1), 156–160.
- (47) Zhao, S.; Ye, Z.; Stanton, R. Misuse of RPKM or TPM normalization when comparing across samples and sequencing protocols. *RNA* **2020**, *26* (8), 903–909.